

Smooth-filamental transition of active tracer fields stirred by chaotic advection

Zoltán Neufeld¹, Cristóbal López² and Peter H. Haynes¹

¹ *Department of Applied Mathematics and Theoretical Physics, University of Cambridge, Silver Street, Cambridge CB3 9EW, UK*

² *Instituto Mediterráneo de Estudios Avanzados, IMEDEA (CSIC-UIB), 07071 Palma de Mallorca, Spain*

(April 26, 2024)

The spatial distribution of interacting chemical fields is investigated in the non-diffusive limit. The evolution of fluid parcels is described by independent dynamical systems driven by chaotic advection. The distribution can be filamental or smooth depending on the relative strength of the dispersion due to chaotic advection and the stability of the chemical dynamics. We give the condition for the smooth-filamental transition and relate the Hölder exponent of the filamental structure to the Lyapunov exponents. Theoretical findings are illustrated by numerical experiments.

The Lagrangian description of fluid flows, considered in the framework of chaotic dynamical systems, has given important insight into mixing and transport [1]. In many situations of practical interest scalar fields describing some property of the fluid are not just simply advected by the flow, but are *active* in the sense that they have their own dynamics, in general coupled to the transport and mixing process. (In the following we will refer to this as the 'chemical' dynamics of the system.) Typical examples of active fields in mixing flows are concentrations of reacting chemicals [2,3] (in industrial processes or the atmosphere) and interacting biological populations of microorganisms in a fluid (e.g. plankton populations stirred by oceanic currents [4]). The spatial structure of such fields often has complex filamental character [5]. Previous work has investigated the temporal evolution of reactions like $A + B \rightarrow C$ or $A + B \rightarrow 2B$ in closed flows [3,6,7] as an initial value problem. The absence of chemical sources in these cases necessarily implies a homogeneous final state of the system. The same reactions were also studied in open chaotic flows [8] where a stationary fractal distribution arises due to the properties of the underlying (chaotic scattering-like) advection dynamics [9]. Here we show that in the case of stable chemical dynamics (in a sense defined below) and in the presence of chemical sources persistent filamental fractal patterns can also arise in closed flows.

The governing equations for a set of N interacting 'chemical' fields C_i mixed by a flow $\mathbf{v}(\mathbf{r}, t)$, independent of the chemical dynamics, can be written as

$$\frac{\partial C_i}{\partial t} + \mathbf{v}(\mathbf{r}, t) \cdot \nabla C_i = \mathcal{F}_i[C_1(\mathbf{r}), \dots, C_N(\mathbf{r}), \mathbf{r}], \quad (1)$$

where $i = 1, \dots, N$. The operators \mathcal{F}_i in general contain

spatial derivatives of the fields C_i , e.g. a Laplacian term representing diffusion.

Let us assume that the advective transport dominates and diffusion is weak. If we neglect non-local processes like diffusion on the right hand side of (1) F_i becomes a simple function of the local concentrations and coordinates. In this case the Lagrangian representation leads to a considerable simplification of the equations, leading to a low-dimensional dynamical system

$$\frac{d\mathbf{r}}{dt} = \mathbf{v}(\mathbf{r}, t), \quad \frac{dC_i}{dt} = F_i(C_1, C_2, \dots, C_N, \mathbf{r}), \quad i = 1, \dots, N, \quad (2)$$

where the second set of equations describes the chemical dynamics inside a fluid parcel that is advected by the flow according to the first equation. The coupling between the flow and chemical evolution is non-trivial if some of the functions F_i depend explicitly on the coordinate \mathbf{r} . In applications this dependence of F_i can appear as a consequence of spatially varying sources, spatially varying (e.g. temperature dependent) reaction rates or reproduction rates of biological species. It is therefore natural to include this dependence in the model to be considered.

Although we use a Lagrangian representation, our aim is to follow not the chemical evolution along individual trajectories, but the spatiotemporal dynamics of the chemical fields $C_i(\mathbf{r}, t)$ that is equivalent to the evolution of the ensemble of fluid parcels under the dynamics (2). Thus the original problem defined in an infinite dimensional phase space is reduced to an ensemble problem in a low-dimensional dynamical system.

By neglecting diffusion, we may miss certain classes of behaviour such as propagating waves, typical for reaction-diffusion systems [10]. However, as we shall see later, we capture a non-trivial behaviour that we believe to be characteristic of the full advection-reaction-diffusion problem when diffusion is weak.

We assume that the flow $\mathbf{v}(\mathbf{r}, t)$ is two-dimensional incompressible and periodic in time with period T . These conditions in general lead to chaotic advection even in case of simple spatially smooth (non-turbulent) velocity fields. Since the advection is independent of the chemical dynamics it can be characterised by its own Lyapunov exponents $\lambda_1^F > \lambda_2^F$. Incompressibility implies that the advection is described by a conservative dynamical system and thus $\lambda_1^F = -\lambda_2^F$.

For numerical investigations we used a simple time-periodic flow that consists of the alternation of two steady sinusoidal shear flows in the x and y direction for the first and the second half of the period, respectively. The flow is defined on the unit square with periodic boundary conditions by the velocity field

$$\begin{aligned} v_x(x, y, t) &= -\frac{U}{T}\Theta\left(\frac{T}{2} - t \bmod T\right) \cos(2\pi y) \\ v_y(x, y, t) &= -\frac{U}{T}\Theta\left(t \bmod T - \frac{T}{2}\right) \cos(2\pi x) \end{aligned} \quad (3)$$

where $\Theta(x)$ is the Heavyside step function. $U \rightarrow 0$ corresponds to an integrable limit of the advection problem. We will consider the case $U = 1.0$ producing a flow that consists of one connected chaotic region. The parameter T controls the relative time-scale of the flow and reactions. By changing T we can vary the Lyapunov exponents of the flow without altering the shape of the trajectories and the spatial structure of the flow.

Since the trajectories $\mathbf{r}(t)$ are chaotic the chemical dynamics (2) corresponds to a chaotically driven dynamical system. This subsystem can be characterised by the set of chemical Lyapunov exponents $\lambda_1^C > \lambda_2^C > \dots > \lambda_N^C$, that depend on the driving by the chaotic advection. Here we will only consider the simplest situation, when the largest chemical Lyapunov exponent is negative and, for a fixed trajectory $\mathbf{r}(t)$, the chemical evolutions converge to the same globally attracting chaotic orbit for any initial condition in the chemical subspace. In the case of no explicit space dependence in the functions F_i (i.e. no driving) this would correspond to a globally attracting fixed point of the chemical subsystem.

A simple example of such a system (relevant for atmospheric photochemistry) is the decay of a chemical species ($N = 1$) produced by a non-homogeneous source, with chemical dynamics

$$\dot{C} = a(\mathbf{r}) - bC, \quad (4)$$

for which $\lambda^C = -b$.

First we investigate the temporal evolution of the chemical fields. Although the Lagrangian variables $C_i(t)$ have a chaotic time-dependence according to the positivity of the largest Lyapunov exponent for the full dynamical system (2), it can be shown that the Eulerian chemical field $C_i(\mathbf{r}, t)$ is asymptotically periodic in time with the period of the flow. In order to obtain the values of the fields at point \mathbf{r} at time t one can *i*) integrate the advection backward in time and use the obtained trajectory $\mathbf{r}(t')$ ($0 < t' < t$) and the initial values of the chemical fields at the point $\mathbf{r}(0)$ to *ii*) integrate the chemical dynamics forward in time from 0 to t . The value of the field at the same point at time $t + nT$ can be obtained similarly. The resulting backward trajectory will be the same (due to the periodicity of the flow) but longer. By integrating the chemical evolution forward in time for nT

we obtain a problem equivalent to the previous one with a different set of initial concentrations, that according to the assumptions made above ($\lambda_1^C < 0$) converge to the same orbit. Consequently the chemical fields are asymptotically periodic in time

$$\lim_{m \rightarrow \infty} C_i(\mathbf{r}, (m+n)T + \tau) = \lim_{m \rightarrow \infty} C_i(\mathbf{r}, mT + \tau), \quad (5)$$

where $\tau = t \bmod T$, defining an asymptotic chemical field $C^\infty(\mathbf{r}, \tau)$.

In the following we investigate the spatial structure of the chemical fields. For this we calculate the difference

$$\delta C_i = C_i(\mathbf{r} + \delta\mathbf{r}, t) - C_i(\mathbf{r}, t), \quad |\delta\mathbf{r}| \ll 1, \quad (6)$$

that can be obtained by integrating (2) along two trajectories ending at the preselected points \mathbf{r} and $\mathbf{r} + \delta\mathbf{r}$ at time t . The time evolution of the distance $|\delta\mathbf{r}(t')|$ (for $t - t' \gg 1$) can be estimated from the time reversed advection dynamics as

$$|\delta\mathbf{r}(t')| \sim |\delta\mathbf{r}(t)| e^{\lambda^F(t-t')} \quad (7)$$

where $\lambda^F = \lambda_1^F > 0$ for almost all final orientations $\mathbf{n}(t) \equiv \delta\mathbf{r}(t)/|\delta\mathbf{r}(t)|$. The only exception is the unstable contracting direction of the time reversed flow corresponding to $\lambda^F = \lambda_2^F < 0$.

By expanding (2) around the chaotic orbit $C_i(\mathbf{r}(t))$ we obtain a set of linear equations

$$\delta\dot{C}_i = \sum_{j=1}^N \frac{\partial F_i}{\partial C_j} \delta C_j + \nabla_r F_i \cdot \delta\mathbf{r} \quad (8)$$

with initial condition

$$\delta C_i(0) = C_i^0(\mathbf{r}(0) + \delta\mathbf{r}(0)) - C_i^0(\mathbf{r}(0)), \quad (9)$$

where $C_i^0(\mathbf{r})$ are the initial chemical fields.

In the simplest case $N = 1$ the solution of (8) can be written explicitly as

$$\delta C(t) = \nabla_r C^0 \cdot \delta\mathbf{r}(0) e^{\lambda t} + \int_0^t \nabla_r F \cdot \delta\mathbf{r}(t') e^{\lambda(t-t')} dt' \quad (10)$$

where

$$\lambda = \frac{1}{t} \int_0^t \frac{\partial F}{\partial C}(C(\mathbf{r}(t')), \mathbf{r}(t')) dt' \quad (11)$$

that becomes equal to the chemical Lyapunov exponent λ^C in the $t \rightarrow \infty$ limit. The first term in (10) represents a deviation due to non-homogeneous initial conditions and the second one describes the effect of different histories of the two trajectories appearing via the space dependence of F .

Using (7) we obtain from (10) for the projection of the gradient of C to a direction \mathbf{n}

$$\frac{\delta C(t)}{|\delta \mathbf{r}(t)|} = \nabla C^0 \mathbf{n}(0) e^{(\lambda^F + \lambda^C)t} + \int_0^t \nabla F(\mathbf{r}(t')) \mathbf{n}(t') e^{(\lambda^F + \lambda^C)(t-t')} dt'. \quad (12)$$

The convergence of the right hand side of the above equation for $t \rightarrow \infty$ depends on the sign of the exponent $\lambda^F + \lambda^C$. If $\lambda^F < |\lambda^C|$ the convergence of the chemical dynamics is stronger than the dispersion of the trajectories in the physical space and results in a smooth field $C^\infty(\mathbf{r}, \tau)$. On the contrary, if $\lambda^F > |\lambda^C|$ the memory of the chemical dynamics decays too slowly to forget the different spatial histories (or initial conditions). In this case the limit does not exist and the field $C^\infty(\mathbf{r}, \tau)$ has an irregular structure that is almost nowhere differentiable. There exists, however, at each point one special direction in which the derivative is finite. This direction is the contracting direction in the time-reversed advection dynamics corresponding to the negative Lyapunov exponent of the flow λ_2^F . Thus we suggest a precise definition of a *filamental* structure, being a non-differentiable field, that is still smooth in one direction at each point (with that direction itself varying smoothly).

The irregular chemical field can be characterised by its Hölder exponent α defined as $\delta C(\delta \mathbf{r}) \sim |\delta \mathbf{r}|^\alpha$, where $0 < \alpha < 1$ and $\alpha = 1$ for a differentiable function. In our case if $\lambda^F + \lambda^C > 0$

$$\delta C(t) \sim |\delta \mathbf{r}(t)| e^{(\lambda^F + \lambda^C)t}. \quad (13)$$

Expressing time from (7) as

$$t = \frac{1}{\lambda^F} \ln \frac{|\delta \mathbf{r}(0)|}{|\delta \mathbf{r}(t)|} \quad (14)$$

and inserting it in (13) we obtain

$$\delta C(t) \sim |\delta \mathbf{r}(0)|^{(1+\lambda^C/\lambda^F)} |\delta \mathbf{r}(t)|^{-\lambda^C/\lambda^F}. \quad (15)$$

For very long times and in a closed flow $|\delta \mathbf{r}(0)|$ will saturate at a finite value in the backward advection dynamics. Thus the Hölder exponent is $\alpha = |\lambda^C|/\lambda^F$. Certainly, diffusion would smooth out the small scale filamental structures below a certain diffusive scale (approaching zero for smaller and smaller diffusivities), setting a cut-off for the scaling relation (15). Nevertheless, above the diffusive scale filamental structures will persist for arbitrarily long time since, in the presence of chemical sources, the effect of diffusion is balanced by the continuous generation of small scale structures by the chaotic advection.

As an example we consider the system (4), which is the simplest possible system that exhibits the smooth-filamental transition, using a source term of the form $a(x, y) = 1 + a_1 \sin(2\pi x) \sin(2\pi y)$. Numerically calculated chemical fields (obtained by a backward integration of the advection problem and forward integration of the chemical dynamics [11]) of both types are shown in

Fig.1a and b. Figure 2 shows a section of the smooth and filamental fields of Fig.1 along the line $y = 0.25$. We also measured the box counting fractal dimension of the function $C(\mathbf{r})$ along a cut in the x direction, which is related to the Hölder exponent by $D = 2 - \alpha$ [12]. Numerically computed values agree well with the theoretical prediction as shown in Fig. 3. If the flow does not consist of only one connected chaotic region, but is composed by chaotic regions separated by KAM tori, the Lyapunov exponents of the flow are different in each chaotic region and the structure of the chemical field can be smooth in certain regions but filamentary in others (Fig 1c.).

In the more general case $N > 1$ the same smooth-filamental transition can be obtained. Let us once again consider at a particular time t the difference $\delta C_i(t)$ in the chemical fields over a small preselected displacement $\delta \mathbf{r}$. The time dependence of a set of initial deviations $\delta C_i(0)$ and $\delta \mathbf{r}(0)$, for the dynamical system (2) has the asymptotic form

$$\left(\sum_{i=1}^N \delta C_i^2(t) + \delta \mathbf{r}^2(t) \right)^{1/2} \sim \left(\sum_{i=1}^N \delta C_i^2(0) + \delta \mathbf{r}^2(0) \right)^{1/2} e^{\lambda t} \quad (16)$$

where λ is one of the Lyapunov exponents of the system. For a typical choice of the final deviation $\delta \mathbf{r}(t)$, $\delta \mathbf{r}$ will be divergent in the time reversed dynamics, and consequently contracting in the forward direction. Thus, the contribution of $\delta \mathbf{r}$ decays in the left hand side of (16) and λ cannot be the positive Lyapunov exponent λ_1^F so the typical value of λ will be the second largest Lyapunov exponent. There are thus two possibilities $\lambda = \lambda_2^F = -\lambda_1^C$ (if $\lambda_2^F > \lambda_1^C$) or $\lambda = \lambda_1^C$ (otherwise). We can now divide both sides of (16) by $\delta \mathbf{r}(t)$ using (7)

$$\left(\sum_{i=1}^N \frac{\delta C_i^2(t)}{\delta \mathbf{r}^2(t)} + 1 \right)^{1/2} \sim \left(\sum_{i=1}^N \frac{\delta C_i^2(0)}{\delta \mathbf{r}^2(0)} + 1 \right)^{1/2} e^{(\lambda_1^F + \lambda)t}. \quad (17)$$

Thus, the chemical fields $C_i(\mathbf{r})$ become non-differentiable in the $t \rightarrow \infty$ limit if $\lambda_1^F > |\lambda_1^C|$.

Numerically we have also observed the smooth-filamental transition in some two-component systems (Brusselator autocatalytic reaction model [13], phytoplankton-zooplankton population dynamics model [14]) for parameters that satisfies the condition $\lambda_1^C < 0$, and obtained distributions very similar to that shown in Fig.1.

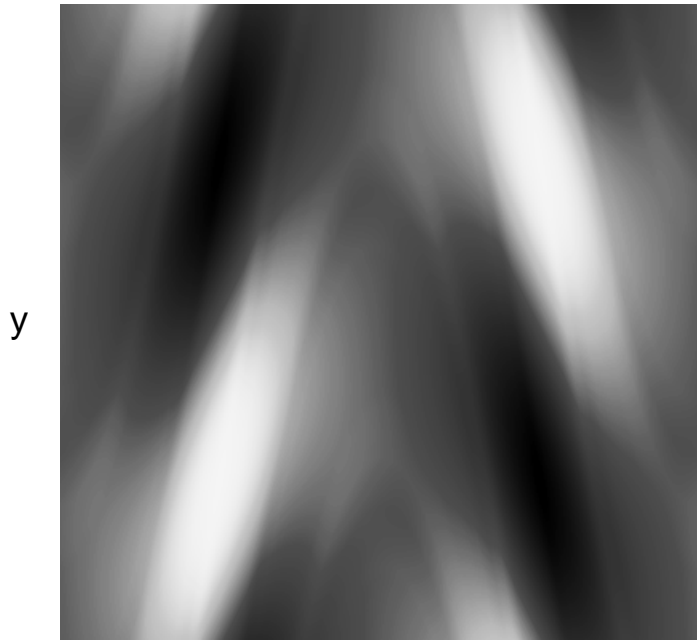
Useful discussions with B. Fernandez, E. Hernández-García and J. Vanneste are acknowledged. Z.N. was funded by a Royal Society-NATO Postdoctoral Fellowship and C.L. was funded by CICYT projects (MAR95-1861) and (MAR98-0840).

- [1] H. Aref, J. Fluid Mech. **143** (1984) 1; J. M. Ottino, *The kinematics of mixing: stretching, chaos and transport*, (Cambridge University Press, Cambridge, 1989); S. Wiggins, *Chaotic transport in dynamical systems*, (Springer-Verlag, 1991); *Chaos applied to fluid mixing* Ed. H. Aref, M. S. El Naschie, (Pergamon/Elsevier, 1995);
- [2] I. R. Epstein, Nature **374**, 321 (1995)
- [3] I. M. Sokolov, A. Blumen, Int. J. Mod. Phys. B **5**(20), 3127 (1991);
- [4] E. R. Abraham, Nature **391**, 577 (1998).
- [5] Edouard et al., Nature **384**, 444 (1996), D. W. Waugh et. al, J. Geophys. Res. **99**, 1071 (1994).
- [6] G. Metcalfe and J.M. Ottino, Phys. Rev. Lett. **72**, 2875 (1994)
- [7] R. Reigada, F. Sagués, I. M. Sokolov, J. M. Sancho and A. Blumen, Phys. Rev. Lett. **78**(4), 741 (1997)
- [8] Z. Toroczkai, Gy. Károlyi, Á. Péntek, T. Tél and C. Grebogi, Phys. Rev. Lett. **80**(3), 500 (1998)
- [9] C. Jung, T. Tél and E. Zemniak, Chaos **3**, 555 (1993); A. Péntek, Z. Toroczkai, T. Tél, C. Grebogi and J.A. Yorke, Phys. Rev. E **51**, 4076 (1995).
- [10] Y. Kuramoto, *Chemical Oscillations, Waves and Turbulence*, (Springer Verlag, Berlin, 1984)
- [11] a similar computational method has been used for the passive tracer problem in F. Városi, M. Antonsen and E. Ott, Phys. Fluids A **3**, 1017 (1991).
- [12] D. L. Turcotte, *Fractals and chaos in geology and geophysics*, (Cambridge University Press, Cambridge, 1997)
- [13] S. K. Scott, *Chemical chaos*, (Oxford University Press, 1991)
- [14] L. Matthews and J. Brindley, Dynamics and Stability of Systems **12**(1), 39 (1997)

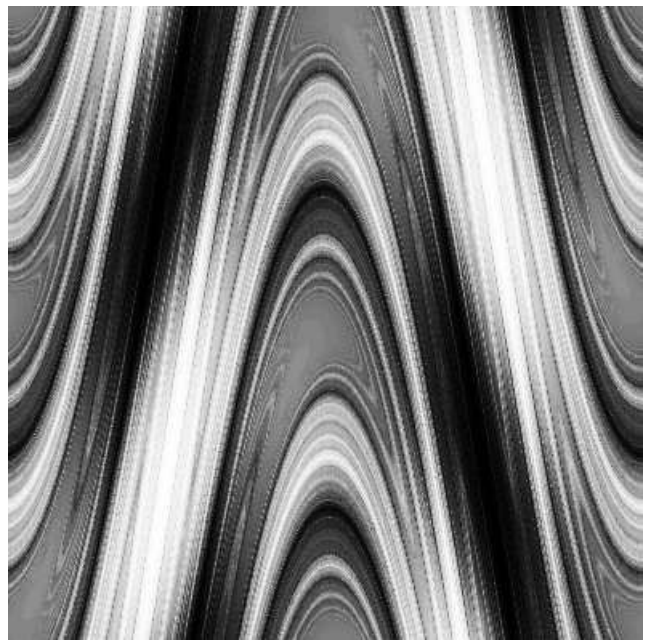
FIG. 1. Smooth (a) and filamental (b) distributions of the decaying substance (eq.4) mixed by the flow (eq. 3) after 20 periods using $a_1 = 0.1$, $b = 1.0$, $U = 1.0$ and initial condition $C(\mathbf{r}, t = 0) = 0.0$. The integration has been done for 200×200 points with final positions on a rectangular grid. For $U = 1.0$ the numerically calculated Lyapunov exponent of the flow is $\lambda^F \approx 2.35/T$. The period of the flow is $T = 5.0$ ($\lambda^F < b$) in (a) and $T = 1.0$ ($\lambda^F > b$) in (b), respectively. (c) coexistence of smooth and filamental structures for $U = 0.5$ and $T = 1.0$.

FIG. 2. Sections of the smooth (a) and filamental (b) fields shown in Fig.1 along the line $y = 0.25$.

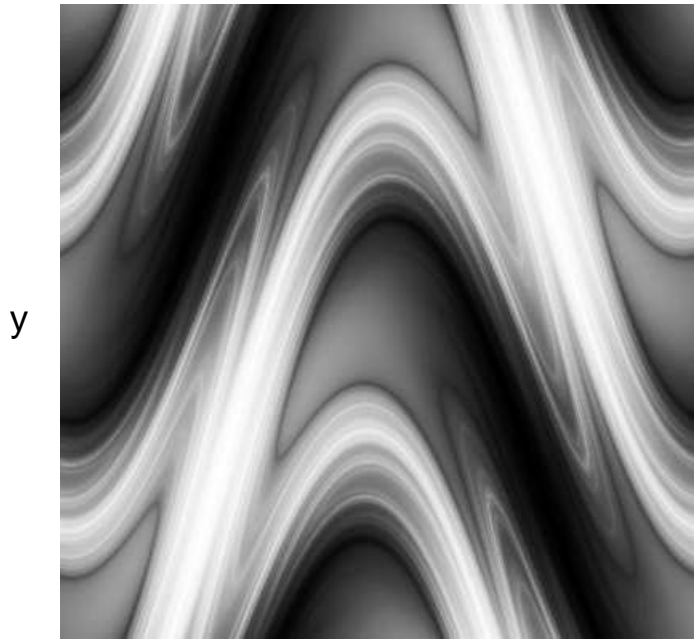
FIG. 3. Box counting fractal dimensions of the functions $C(x)$ shown in Fig.2. Number of boxes needed to cover the graph of the function $C(x)$ vs. the box size l (squares) and slopes corresponding to the relation $D = 2 - b/\lambda^F$.



(a)



(b)



(c)

